COORDINATE-INDEPENDENT ANGLE-GATHERS FOR WAVE-EQUATION MIGRATION

FOURIER-DOMAIN IMAGING CONDITION

The imaging condition (2) can also be formulated in the Fourier domain similarly to the approach of Artman and Fomel (2005). In the Fourier domain, we can write

(25)

$$\widehat{\mathbf{R}}(\mathbf{k_m},\mathbf{k_h}) = \frac{1}{2}\sum_s \hat{\mathbf{u}}_s\left(\frac{\mathbf{k_m}-\mathbf{k_h}}{2},\omega\right)\hat{\mathbf{u}}_r^*\left(\frac{\mathbf{k_m}+\mathbf{k_h}}{2},\omega\right)$$

where $\widehat{\ }$ stands for a Fourier transform, and * for complex conjugate. The image R_0 is obtained using an inverse Fourier transform over $\mathbf{k_m}$ of the image constructed using equation (25), after summation over the offset wavenumbers $\mathbf{k_h}$:

(26)

$$\mathbf{R}_0(\mathbf{m}) = \mathtt{IFT}\sum_{\mathbf{k_h}} \widehat{\mathbf{R}}(\mathbf{k_m},\mathbf{k_h})$$

An intriguing possibility is raised by the following construction: the image constructed using equation (25) is formulated in the $\mathbf{k_m}$, $\mathbf{k_h}$ Fourier domain; the angle-mapping formula (13) is also written in the Fourier domain; therefore, using equations (25) and (13), we can construct a second image based on the following formula:

(27)

$$\widehat{\mathbf{R}}_\theta(\mathbf{k_m},\mathbf{k_h}) = \widehat{\mathbf{R}}(\mathbf{k_m},\mathbf{k_h})\frac{|\mathbf{k_h}|}{|\mathbf{k_m}|}$$

This image can also be transformed to the space domain using summation over the offset wavenumbers $\mathbf{k_h}$ and inverse Fourier transform over the space coordinates

(28)

$$\mathbf{R}_\theta(\mathbf{m}) = \mathtt{IFT}\sum_{\mathbf{k_h}} \widehat{\mathbf{R}}_\theta(\mathbf{k_m},\mathbf{k_h})$$

Then, using equations (26) and (28), we can obtain the reflection angle field $\tan\theta(\mathbf{m})$ using a simple division of the two images:

(29)

$$\tan\theta(\mathbf{m}) = \frac{\mathbf{R}_\theta(\mathbf{m})}{\mathbf{R}_0(\mathbf{m})}$$

analogously to methodology employed by Bleistein et al. (2000) to Kirchhoff imaging. The reflection angle field $\tan\theta$ (**m**) describes the angle at which one particular shot illuminates the image R_0 (**m**). The final image is obtained by summation of all such images constructed for independent shots, with contribution of different shots added at their respective angle. This approach substantially reduces the storage requirements for shot-record migration, while still producing angle-dependent reflectivity. A similar procedure can be used to encode the reflection azimuth field $\cos\phi$ (**m**) instead of the reflection angle field $\tan\theta$ (**m**), by using equation (24) as the scale factor in equation (27).

Figure 2

Geometry of the experiments depicted in Figures 3–6. In all cases, x_{CIG} = 3000m and z_{CIG} = 1200m. The structural dip α and reflection θ angles change for every figure. The source location changes in every figure according to the dip and reflection angles.

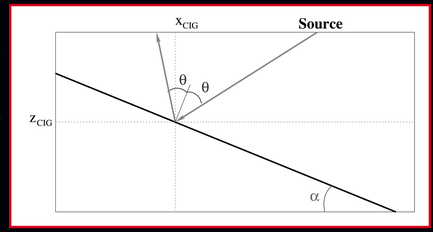

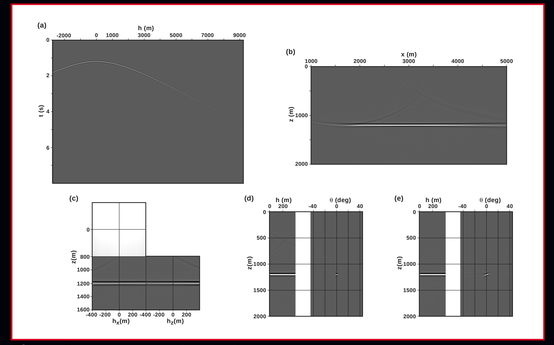

Figure 3 Experiment 1: α = 0° and θ = 0°.

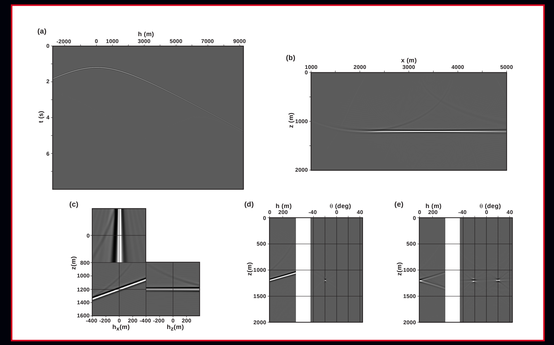

Figure 4 Experiment 2: α = 0° and θ = 20°.

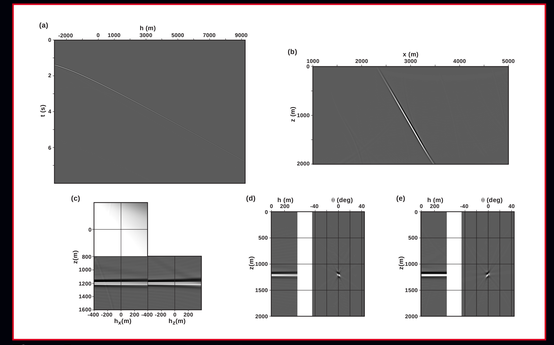

Figure 5 Experiment 3: α = 60° and θ = 0°.

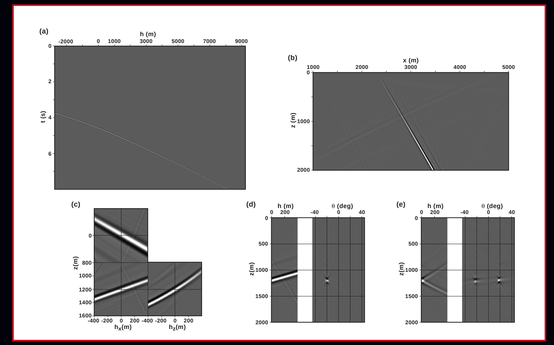

Figure 6 Experiment 4: α = 60° and θ = 20°.

EXAMPLE

Figures 2–6 illustrate the angle decomposition described in this paper with a simple synthetic example. The geometry of the experiment is described in Figure 2. In all cases, the source location changes according to the structural dip angle α and reflection angle θ.

The panels in Figures 3–6 depict the following:

- The data recorded on the surface. The offset range changes according to the geometry of the experiment.
- The migrated image using wavefield extrapolation.
- A multi-offset cube at the image location (x_{CIG}) function of depth (z), and the two components of the offset vector (h_X and h_Z).
- Angle decomposition based on the horizontal offset (h_X) using equation (19).
- Angle decomposition based on the full offset vector (h) using equation (13).

CONCLUSION

We implement coordinate-independent angle decomposition for images constructed using migration by wavefield extrapolation. This transformation involves computing 3-D offset vectors h during the imaging step. This requirement adds more computations, since more cross-correlations are required. However, the storage requirements for reflection angle imaging is decreased, since the transformation depends on the absolute magnitude of the offset vector ($|\mathbf{k_h}| = k_{|\mathbf{h}|}$), rather than on its components. Azimuth analysis requires storage of all offset vector components.

REFERENCES

Artman, B., and Fomel, S., 2005, Fourier domain imaging condition for shot-profile migration *in* 75th Ann. Internat. Mtg. Soc. of Expl. Geophys.

Biondi, B., 2002, Stable wide-angle Fourier finite-difference downward extrapolation of 3-D wavefields: Geophysics, 67, 872–882.

Biondi, B., and Shan, G., 2002, Prestack imaging of overturned reflections by reverse time migration *in* 72nd Ann. Internat. Mtg. Soc. of Expl. Geophys., 1284–1287.

Biondi, B., and Symes, W. W., 2004, Angle-domain common-image gathers for migration velocity analysis by wavefield-continuation imaging: Geophysics, 69, 1283–1298.

Bleistein, N., Cohen, J., and Stockwell, J., 2000, Mathematics of multidimensional seismic imaging, migration, and inversion: Springer.

Brandsberg-Dahl, S., and Etgen, J., 2003, Beam-wave migration: 65th Mtg., Eur. Assoc. Geosc. Eng., Abstracts.

de Bruin, C. G. M., Wapenaar, C. P. A., and Berkhout, A. J.,1990, Angle-dependent reflectivity by means of prestack migration: Geophysics, 55, 1223–1234.

Cervený, V., 2001, Seismic ray theory: Cambridge Univ. Press.

Claerbout, J. F., 1985, Imaging the Earth's Interior: Blackwell Scientific Publications.

Etgen, J., 2002, Waves, beams and dimensions: an illuminating if incoherent view of the future of migration: 72nd Ann. Internat. Mtg, Soc. of Expl. Geophys.

Fomel, S., 2004, Theory of 3-D angle gathers in wave-equation imaging *in* 74th Ann. Internat. Mtg. Soc. of Expl. Geophys.

Gray, S. H., Etgen, J., Dellinger, J., and Whitmore, D., 2001, Seismic migration problems and solutions: Geophysics, 66, 1622–1640.

Hale, D., Hill, N. R., and Stefani, J., 1992, Imaging salt with turning seismic waves: Geophysics, 57, 1453–1462.

Hill, N. R., 2001, Prestack Gaussian-beam depth migration: Geophysics, 66, 1240–1250.

de Hoop, M. V., 1996, Generalization of the Bremmer coupling series *in* J. Math. Phys. 3246–3282.

Huang, L. Y., and Wu, R. S., 1996, Prestack depth migration with acoustic screen propagators *in* 66th Ann. Internat. Mtg. Soc. of Expl. Geophys., 415–418.

Mosher, C., and Foster, D., 2000, Common angle imaging conditions for prestack depth migration *in* 70th Ann. Internat. Mtg. Soc. of Expl. Geophys., 830–833.

Prucha, M., Biondi, B., and Symes, W., 1999, Angle-domain common image gathers by wave-equation migration *in* 69th Ann. Internat. Mtg. Soc. of Expl.Geophys., 824–827.

Rickett, J. E., and Sava, P. C., 2002, Offset and angle-domain common image-point gathers for shot-profile migration: Geophysics, 67, 883–889.

Ristow, D., and Ruhl, T., 1994, Fourier finite-difference migration: Geophysics, 59, 1882–1893.

Sava, P., and Fomel, S., 2004, Riemannian wavefield extrapolation *in* 74th Ann. Internat. Mtg. Soc. of Expl. Geophys.

–, 2005, Wave-equation common-angle gathers for converted waves *in* 75th Ann. Internat. Mtg. Soc. of Expl. Geophys.

Sava, P. C., and Fomel, S., 2003, Angle-domain common- image gathers by wavefield continuation methods: Geophysics, 68, 1065–1074.

Shan, G., and Biondi, B., 2004, Imaging overturned waves by plane-wave migration in tilted coordinates: SEG Technical Program Expanded Abstracts, 23, 969–972.

Soubaras, R., 2003, Angle gathers for shot-record migration by local harmonic decomposition *in* 73rd Ann. Internat. Mtg. Soc. of Expl. Geophys., 889–892.

Xie, X., and Wu, R., 2002, Extracting angle domain information from migrated wavefield *in* 72nd Ann. Internat. Mtg. Soc. of Expl. Geophys., 1360–1363.